The Journal of Immunology

Antigen-Specific Suppression of Inflammatory Arthritis Using Liposomes

Christelle Capini, Montree Jaturanpinyo, Hsin-I Chang, Srinivas Mutalik, Alice McNally, Shayna Street, Raymond Steptoe, Brendan O'Sullivan, Nigel Davies and Ranjeny Thomas

---

References   This article **cites 38 articles**, 24 of which you can access for free at:
http://www.jimmunol.org/content/182/6/3556.full#ref-list-1

Why *The JI*? Submit online.

- **Rapid Reviews! 30 days*** from submission to initial decision

- **No Triage!** Every submission reviewed by practicing scientists

- **Fast Publication!** 4 weeks from acceptance to publication

average

Antigen-Specific Suppression of Inflammatory Arthritis Using Liposomes[1]

Christelle Capini,* **Montree Jaturanpinyo,[2]†** **Hsin-I Chang,†** **Srinivas Mutalik,†**
Alice McNally,* **Shayna Street,*** **Raymond Steptoe,*** **Brendan O'Sullivan,*** **Nigel Davies,†**
and Ranjeny Thomas[3]*

Existing therapies for rheumatoid arthritis and other autoimmune diseases are not Ag specific, which increases the likelihood of systemic toxicity. We show that egg phosphatidylcholine liposomes loaded with Ag (OVA or methylated BSA) and a lipophilic NF-κB inhibitor (curcumin, quercetin, or Bay11-7082) suppress preexisting immune responses in an Ag-specific manner. We injected loaded liposomes into mice primed with Ag or into mice suffering from Ag-induced inflammatory arthritis. The liposomes targeted APCs in situ, suppressing the cells' responsiveness to NF-κB and inducing Ag-specific FoxP3$^+$ regulatory T cells. This regulatory mechanism suppressed effector T cell responses and the clinical signs of full-blown Ag-induced arthritis. Thus, liposomes encapsulate Ags and NF-κB inhibitors stably and efficiently and could be readily adapted to deliver Ags and inhibitors for Ag-specific suppression of other autoimmune and allergic diseases. *The Journal of Immunology,* 2009, 182: 3556–3565.

T he clinical manifestations of rheumatoid arthritis (RA)[4] respond well to disease-modifying and biologic agents but therapies currently on the market are not Ag specific, which increases the likelihood of systemic toxicity. RA treatment fails in up to 50% of patients because of adverse effects or because the therapy does not work (1, 2). The ability to formulate an effective therapy for a patient displaying a specific autoimmune reactivity would reduce the expensive and potentially dangerous trial and error currently involved in RA treatment.

Autoimmune rheumatic diseases result from a break in self-tolerance, development of chronic inflammation, and, ultimately, tissue destruction. In RA, a number of autoantibodies are described, including rheumatoid factor and the highly disease-specific anti-citrullinated peptide Abs. These Abs are found in 70% of patients (3). Dendritic APCs (DCs) contribute to this inflammatory process by priming au-

toreactive responses in the periphery and by thymic shaping of the T cell repertoire through deletion of autoreactive thymocytes (4, 5).

In previous work, we used the NF-κB inhibitor Bay11-7082 to inhibit the maturation of DCs (6, 7). After application of NF-κB inhibitors, DCs generated from bone marrow or peripheral blood precursors ex vivo expressed fewer CD40 and MHC class II molecules and only weakly stimulated proliferation and IFN-γ production by T cells (7, 8). These DCs, when exposed to Ag and injected into mice, suppressed previously primed immune responses, including full-blown inflammatory arthritis, through the induction of Ag-specific regulatory CD4$^+$ T cells (Treg cells). Experiments in knockout mice showed that the RelB subunit of NF-κB expressed by DCs controlled the outcome of Ag presentation to T cells and that Ag-specific Treg cells induced by RelB^{low} DCs produced IL-10 and induced tolerance when transferred from one animal to another (7, 9).

In the current study, we exploited the useful immunomodulatory properties of RelB^{low} DCs using a cell-free approach in which liposomes deliver a payload of Ag and NF-κB inhibitor to APCs in vivo. This system has the potential to overcome the prohibitively high cost and difficulties in manufacture that prevent use of RelB^{low} DCs for therapy of large numbers of patients.

Materials and Methods

Mice

C57BL/6 and BALB/c mice were housed in specific pathogen-free conditions and were supplied by the Animal Research Centre (Perth, Australia). The OVA-specific TCR-transgenic mouse strains, D011.10 on the BALB/c background and OT-II on the C57BL/6 background, were bred at the University of Queensland.

Liposome formulation

Bay 11-7082 was obtained from BIOMOL; curcuminoids, comprising curcumin, demethoxycurcumin, and bis-demethoxycurcumin (94% purity, analytical grade), were a gift from Synthite Industrial Chemicals. Quercetin, OVA, and methylated BSA (mBSA) were purchased from Sigma-Aldrich. Liposomes containing NF-κB inhibitor and Ag were prepared by lipid film hydration. Briefly, egg phosphatidylcholine (EPC; Northern Lipids) and NF-κB inhibitor were dissolved together in chloroform/ethanol and evaporated to produce a thin film under reduced pressure in a rotary evaporator.

OVA or mBSA Ag was added and shaken. The resulting liposomes were subjected to five cycles of freezing and thawing. Liposomes were extruded through 400-nm polycarbonate membranes (Nucleopore) at ambient temperature, then centrifuged to remove nonentrapped materials. Liposomes were redispersed in HEPES buffer (pH 7.4), stored at 4°C, and used within 7 days of preparation. The final concentration of liposomal OVA was 2 mg/ml, mBSA was 2.5 mg/ml, Bay11-7082 was 0.5 mM, curcumin was 2 mM, and quercetin was 2 mM. The presence of NF-κB inhibitors in the liposomes did not affect their capacity to entrap OVA and mBSA. For some experiments, liposomes were fluorescently labeled by adding ethanolic stock of 1,1′-dioctadecyl-3,3,3′,3′-tetramethylindocarbocyanine perchlorate (DiI) or 1,1′-dioctadecyl-3,3,3′,3′-tetramethylindotricarbocyanine iodide (DiR) (Invitrogen/Molecular Probes) to extruded liposome dispersions (10).

In vivo and ex vivo imaging

C57BL/6 mice were injected i.v. with 100 μl of DiR-labeled liposomes. Two hours later, the mice were sacrificed and imaged with a Kodak Imaging Station, combining multi-wavelength and x-ray imaging. Excised inguinal lymph nodes (LNs), mesenteric LNs, and spleen were subsequently imaged.

In vivo fate of liposomes following i.v. or s.c. administration

One hundred microliters of liposomes were injected i.v. or s.c. at the tail base into C57BL/6 mice. Twenty-four hours later, spleen, inguinal, mesenteric, and axillary LNs were removed and pressed through a cell strainer. Cell suspensions were stained with anti-mouse MHC class II-FITC, anti-CD11c-allophycocyanin, anti-CD8-FITC, anti-B220-FITC, or anti-F480-allophycocyanin (BioLegend) before analysis by flow cytometry.

Microscopy

The spleens of untreated mice or i.v. DiI-curcumin liposome-injected C57BL/6 mice were harvested, embedded in OCT compound, and snap frozen. Seven-micrometer cryosections were fixed in ice-cold acetone (Sigma-Aldrich) for 10 min and dried at room temperature. Sections were stained at room temperature with either anti-CD11c-Alexa Fluor 647 and anti-CD8Alexa Fluor 488, anti-CD11c-Alexa Fluor 647 and anti-F480-Alexa Fluor 488, anti-CD11b-Alexa Fluor 647 and anti-F480-Alexa Fluor 488 or anti-CD11c-Alexa Fluor488 (all from BioLegend) and anti-PDCA1-allophycocyanin (Miltenyi Biotec). No red background staining was observed in spleens of PBS-injected mice (data not shown). Slides were washed three times in PBS, mounted with OCT mounting medium, and imaged on an ApoTome microscope (Zeiss). Splenocytes from mice injected with liposomes were treated with or without LPS and stained with NF-κB-p50 Ab (Santa Cruz Biotechnology), then with Alexa Fluor 488 goat anti-rabbit IgG (Invitrogen) and finally 4′,6-diamidino-2-phenylindole. Cells were imaged by confocal microscope using a ×63 objective (Zeiss).

NF-κB binding ELISA

Groups of C57BL/6 mice ($n = 3$) were injected i.v. with 100 μl of liposomes containing quercetin or curcumin and OVA. Control mice received either i.v. injections of empty or OVA liposomes or were primed with OVA in CFA (Sigma-Aldrich). After 24 h, splenocytes were prepared and incubated for 24 h with or without 100 ng/ml LPS in RPMI 1640 medium containing 10% FCS. Nuclear extracts were prepared as described previously (11). p50/NF-κB DNA binding was detected by ELISA using a BD Transfactor Family Colorimetric kit (BD Biosciences) as described elsewhere (6). The resulting color was detected by a Multiskan plate reader (Labsystems).

Tolerance induction

CFSE dilution. Spleen and LN cells from naive DO11.10 mice were labeled in 10 μM CFSE (Invitrogen). Cells (5×10^6) were injected i.v. into each recipient BALB/c mouse. After 24 h, 100 μl of liposome formulations were injected s.c. into groups of five mice. Inguinal LN cells were stained with clonotypic KJ1-26 mAb (BD Pharmingen) 72 h later and analyzed by flow cytometry.

OVA-specific responses. After injection of splenocytes and LN cells from naive OVA-specific TCR-transgenic DO11.10 mice, recipient BALB/c mice were primed with OVA-CFA. Seven days later, mice were injected s.c. with 100 μl of liposome formulations coentrapping OVA with or without NF-κB inhibitor. After 7 days, T cells were enriched from inguinal LN cells by nylon wool columns. In brief, 10^5 T cells were incubated for 3 days in round-bottom wells with 2×10^5 CD11c$^+$ DCs purified from spleens of naive BALB/c mice by positive immunoselection (Miltenyi Biotec) in the presence of OVA$_{323-339}$ peptide (Auspep) at concentrations be-

tween 0 and 1000 ng/ml. Cells were pulsed for the final 18 h of culture with [^{3}H]thymidine. Proliferation is reported as the mean cpm ± SEM of triplicate wells. IFN-γ, IL-2, IL-10, TNF, and IL-6 were measured in supernatants using the BD Cytometric Bead Array Mouse Inflammation Kit (BD Pharmingen).

Transfer of tolerance. In brief, 10^6 OVA-specific TCR-transgenic OT-II T cells per mouse were transferred i.v. to C57BL/6 mice which were to serve as T cell donors. After 24 h, these mice were injected s.c. with liposomes coentrapping curcumin and OVA, curcumin and mBSA, or they were left untreated. A second group of recipients was primed with OVA-CFA. After 7 days, T cells were purified from each donor group. In brief, 10^6 T cells/mouse were injected into each primed recipient, maintaining five recipients per liposome treatment group. After 24 h, all recipient groups were boosted with OVA-CFA. After 7 days, OVA-specific inguinal LN T cell responses were measured as described above.

Detection and depletion of Treg cells. In brief, 10^6 OVA-specific TCR-transgenic DO11.10 T cells per mouse were transferred i.v. to BALB/c mice. After 24 h, these mice were primed s.c. with 100 μl of OVA-CFA. Seven days later, the mice were injected s.c. with either: OVA-liposomes, OVA-Bay-DCs, OVA-Bay-liposomes, OVA-curcumin-liposomes, mBSA-curcumin-liposomes, or Bay solution, and one group was untreated. After 8 days, the inguinal LN cells of each group were pooled, purified, and stained with anti-CD4 PE, anti-CD25-FITC, and anti-FoxP3 allophycocyanin (each from BioLegend), then analyzed by flow cytometry.

DO11.10 T cells were adoptively transferred into two groups of BALB/c mice on day 0. Group 1 received CD4$^+$ T cells and group 2 received CD25$^-$CD4$^+$ DO11.10 T cells (purified by MACS; Miltenyi Biotec). Group 2 was treated with 0.75 mg of anti-CD25 mAb (PC61, rat IgG1; American Type Culture Collection) on days −1, 2, and 7. On day 1, mice from each group were treated s.c. with either no treatment, OVA-curcumin-liposomes, or mBSA-curcumin-liposomes. On day 8, all groups were primed with OVA-CFA. Seven days after priming, T cells were purified from draining inguinal LNs and restimulated with OVA peptide as described above. CD25$^+$FoxP3$^+$ cells were identified in inguinal LNs by flow cytometry as described above.

Ag-induced inflammatory arthritis (AIA) model. Twenty-one days before arthritis induction, C57BL/6 mice were immunized in each axilla by intradermal injection of 100 μg of mBSA emulsified in CFA. Simultaneously, 400 ng of pertussis toxin was injected i.p. Seven days later, a booster dose of 100 μg of mBSA-CFA was delivered s.c. Arthritis was induced by intra-articular injection of 60 μg of mBSA into the right knee joint cavity (day 0), while the control left knee joint was treated with saline. On day 7, each group of mice ($n = 10$) was injected s.c. with 100 μl of liposomal formulations at the tail base. Control mice were either untreated or received curcumin-liposomes administered concurrently with 125 μg of mBSA s.c. From the day of arthritis induction, knee joint swelling was measured in each mouse every 3–4 days for 10–13 days with a Vernier caliper (Mitutoyo) and then expressed as a percentage based on the difference between the diameters of the right and the left knee joint, where the maximum difference between two knees in each mouse was equal to 100%. At day 13, after sacrifice, the knee skin was removed. Severity of knee joint swelling was compared between knees injected with Ag and saline and expressed as a clinical score. The score was rated from 1 to 5, where 1 = no change between saline and Ag knees, 2 = slight discoloration of joint, 3 = discoloration of joint and mild lateral swelling and discoloration, 4 = discoloration of joint and moderate lateral swelling and discoloration, and 5 = severe discoloration of joint to the point where the ligament is no longer visible and severe lateral swelling and discoloration are apparent. All scoring was conducted without knowledge of treatment group.

Statistical analysis

Significant differences between groups of data were determined either by an unpaired Student's *t* test (where two comparisons were being made) or ANOVA (where multiple comparisons were being made). A value of $p < 0.05$ was considered to indicate a significant difference.

Results

NF-κB inhibitors incorporated into liposomes were Bay11-7082 (7, 12), curcumin, and quercetin. Curcumin is a phenolic natural product isolated from the rhizome of *Curcuma longa* (turmeric). It has anti-inflammatory, antimutagenic, and antioxidant properties attributed to inhibition of signal transduction pathways, e.g., p38

MAPK and NF-κB (13). Quercetin is a major flavonoid found in fruits such as apricots and mangoes, with similar therapeutic properties to curcumin (14). Liposomes coentrapping these NF-κB inhibitors and OVA and mBSA Ags were prepared.

Traffic and uptake of liposomes

Liposomes were labeled with DiI or DiR because of their strong fluorescence, low toxicity, and because they integrate with high stability into the liposome and remain fixed there even when in contact with other membranes (10). Two hours after i.v. administration of DiR-labeled EPC liposomes to mice, distribution was determined by in vivo imaging. Intense DiR fluorescence was observed in lymphoid organs of the reticuloendothelial system, especially spleen and mesenteric LNs (Fig. 1).

To assess the cellular fate of the liposomes arriving in lymphoid organs 24 h after injection of the mice, we examined spleens after i.v. injection and inguinal draining LNs after s.c. injection with DiI-labeled liposomes. Cell suspensions from these organs were examined by flow cytometry or complete organs were embedded, sectioned, and examined by immunofluorescence microscopy. DiI-liposomes were taken up almost exclusively by MHC class II^{+} cells in spleens and inguinal LNs (Fig. 2*A*). The fraction of APCs containing liposomes was negligible in nondraining axillary LNs (data not shown). Immunofluorescence microscopy and flow cytometric analysis indicated that liposomes were taken up by F480^{+} and CD11b^{+} macrophages and DCs and CD11c^{+} myeloid and plasmacytoid DCs, including B220^{high}CD11c^{low} and B220^{low} CD11c^{high} subsets (Fig. 2*B*), PDCA1^{+} and PDCA1^{−}CD11c^{+} DCs (Fig. 2*E*, white and yellow arrows, respectively), and CD8^{+} and CD8^{−} DC subsets (Fig. 2, *C* and *E*, white and yellow arrows, respectively) (15–19).

Suppression of NF-κB activity in lymphoid organs of mice after uptake of liposomes formulated with NF-κB inhibitors

To determine whether NF-κB activity was suppressed after liposome uptake in vivo, mice were injected i.v. with either empty liposomes, liposomes entrapping OVA, or liposomes coentrapping OVA and either curcumin or quercetin. After 24 h, splenocytes were isolated and incubated with or without LPS, a TLR agonist that induces NF-κB signaling. After another 24 h, cell nuclei were extracted and ELISA was used to determine p50/NF-κB DNA binding to consensus oligonucleotides. Nuclear p50 was chosen as a binding target because it is highly expressed by APCs and was therefore considered a sensitive readout of NF-κB activity. In the absence of LPS, p50 DNA binding was low in all nuclear extracts. Stimulation with LPS ex vivo increased p50 DNA binding 2-fold in nuclei from mice treated with empty liposomes or OVA-containing liposomes. In contrast, LPS did not stimulate p50 DNA binding in nuclei from mice injected with liposomes entrapping quercetin or curcumin (Fig. 3*A*).

We confirmed these observations by confocal microscopy of splenocytes cultured with or without LPS 24 h after injection of DiI-labeled liposomes or DiI-labeled curcumin liposomes. After injection of liposomes or curcumin liposomes, splenocytes contained cytoplasmic NF-κB-p50. However, after incubation with LPS, translocation of NF-κB-p50 to the nucleus was only observed in splenocytes isolated from mice injected with DiI-labeled liposomes (Fig. 3*B*).

Liposomal delivery of Ag to T cells in draining LNs

We next determined whether liposomes delivered Ag to APCs and that the APCs could then deliver this Ag to Ag-specific T cells in lymphoid organs. Liposomes entrapping OVA (with or without NF-κB inhibitors) were injected s.c. into naive mice, to which
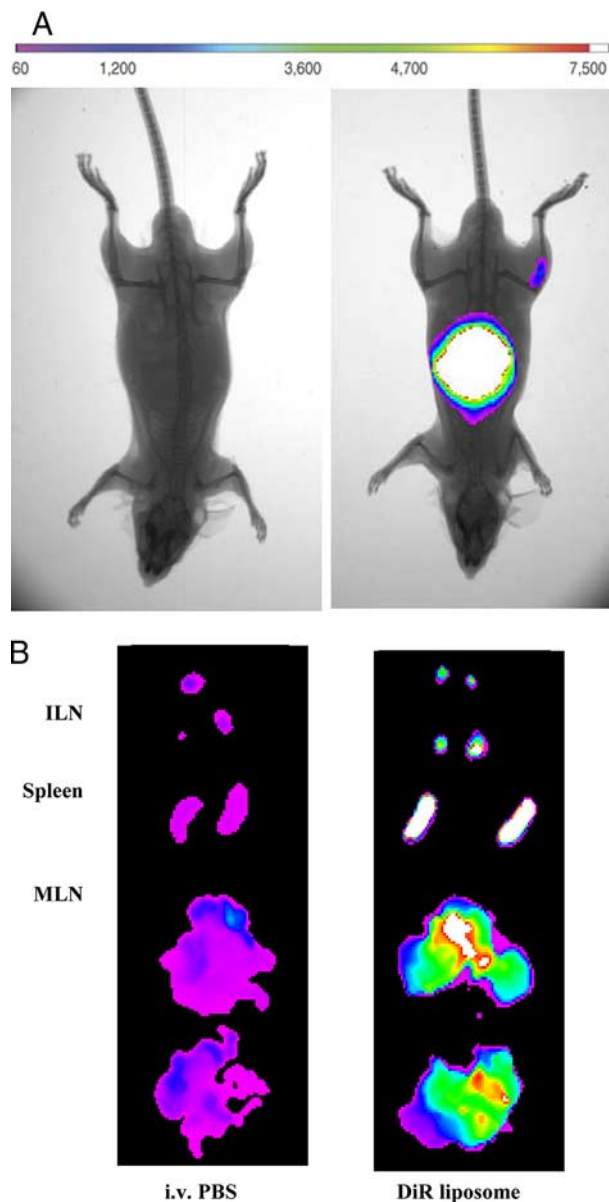

FIGURE 1. Liposomes traffic to the reticuloendothelial system after i.v. injection. Two hours after i.v. DiR-labeled curcumin-liposome injection, intact mice (*A*) or inguinal LNs (ILN), mesenteric LNs (MLN), and spleen removed from those mice (*B*) were subjected to combined multi-wavelength and x-ray imaging. Mice injected with PBS were imaged as controls.

CFSE-labeled OVA-specific TCR-transgenic T cells had been adoptively transferred. Draining LN cells were recovered 72 h later. To measure Ag-specific T cell proliferation, we used flow cytometry to analyze cells expressing the clonotypic KJ1-26 mAb for CFSE dilution. Empty liposomes did not induce T cell proliferation. T cells divided vigorously in all other mice (Fig. 4). Thus, liposomes effectively delivered Ag to APCs in vivo and stimulated T cell proliferation. This T cell response to OVA delivered along with a NF-κB inhibitor is supported by previous findings of a strong, Ag-dependent T cell proliferation in response to Ag, which occurs at early time points only to subside at later time points when Ag is presented under tolerogenic conditions (20–24).

Priming of Ag-specific Treg cells in response to liposomes entrapping curcumin and Ag

To test whether liposomes coentrapping OVA and a NF-κB inhibitor induced Ag-specific tolerance, naive mice were primed with
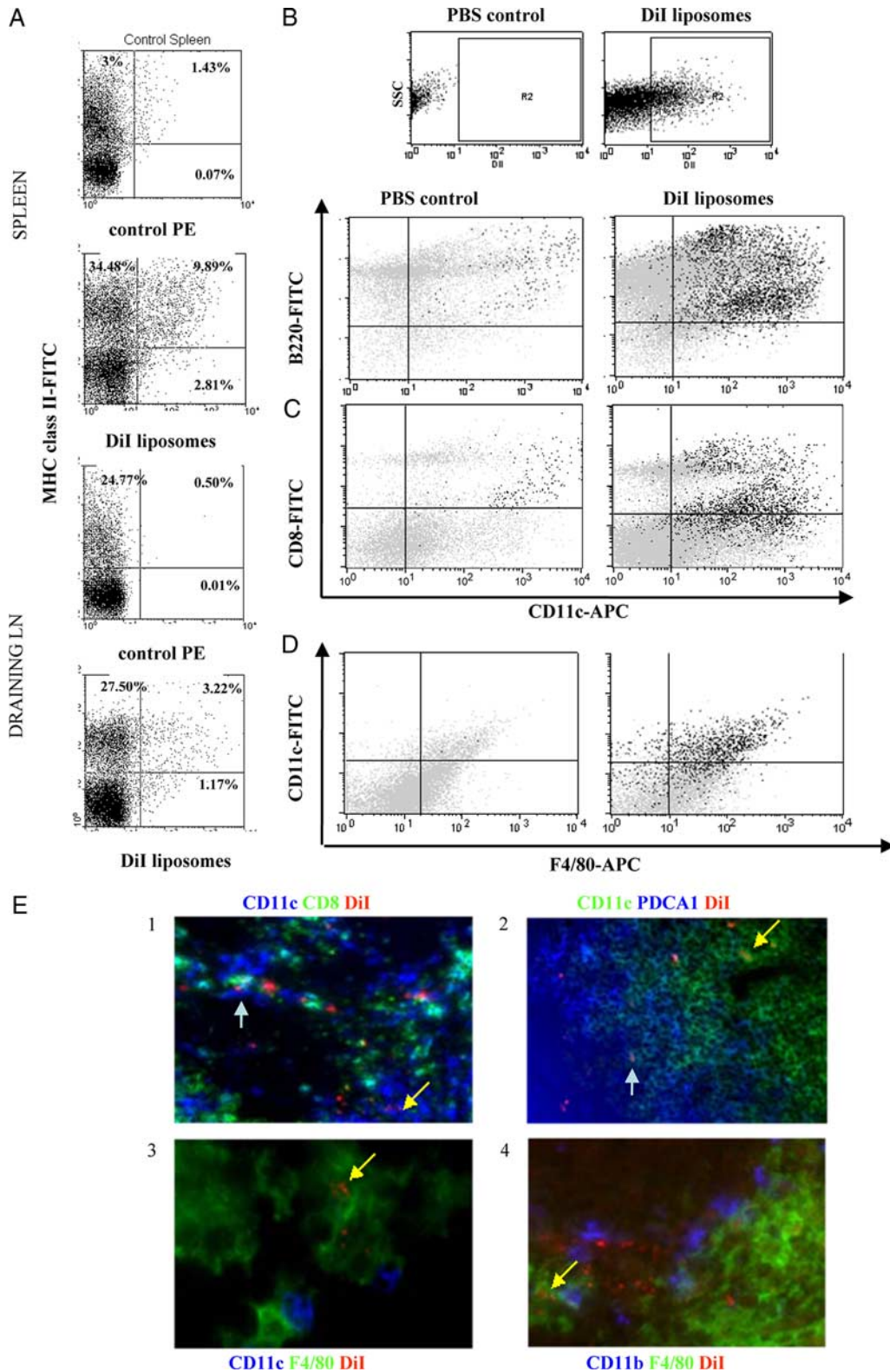
FIGURE 2. DiI-labeled curcumin-liposomes are taken up by macrophages and DCs. Twenty-four hours after injection, spleen of C57BL/6 mice injected i.v. and inguinal draining LNs of mice injected s.c. with DiI-labeled (red fluorescence) curcumin-liposomes or PBS were removed. Cells from each organ were stained with anti-MHC class II FITC (*A*). After s.c. injection of DiI-labeled liposomes, draining LN cells were stained with anti-CD11c allophycocyanin, anti-CD8 FITC, anti-B220-FITC, or anti-F480 allophycocyanin and analyzed by flow cytometry. Red fluorescent cells were gated as shown (R2) and appear in black in each plot (*B–D*). After i.v. injection of DiI-labeled liposomes, frozen spleens were stained as shown with anti-CD11c Alexa Fluor 647 and anti-CD8 Alexa Fluor 488 (LN; original magnification, ×40), anti-CD11c Alexa Fluor 488 and anti-PDCA1 allophycocyanin (spleen; original magnification, ×20), anti-CD11c Alexa Fluor 647 and F480 Alexa Fluor 488 (spleen; original magnification, ×63), and anti-CD11b Alexa Fluor 647 and F480 Alexa Fluor 488 (LN; original magnification, ×40 resolution) (*E*). Examples of liposomes (red) located to DCs or macrophages single labeled with either CD11c or F4/80 are identified with yellow arrows and those located to DCs double labeled with either CD11c and CD8 or CD11c and PDCA1 are identified with white arrows.
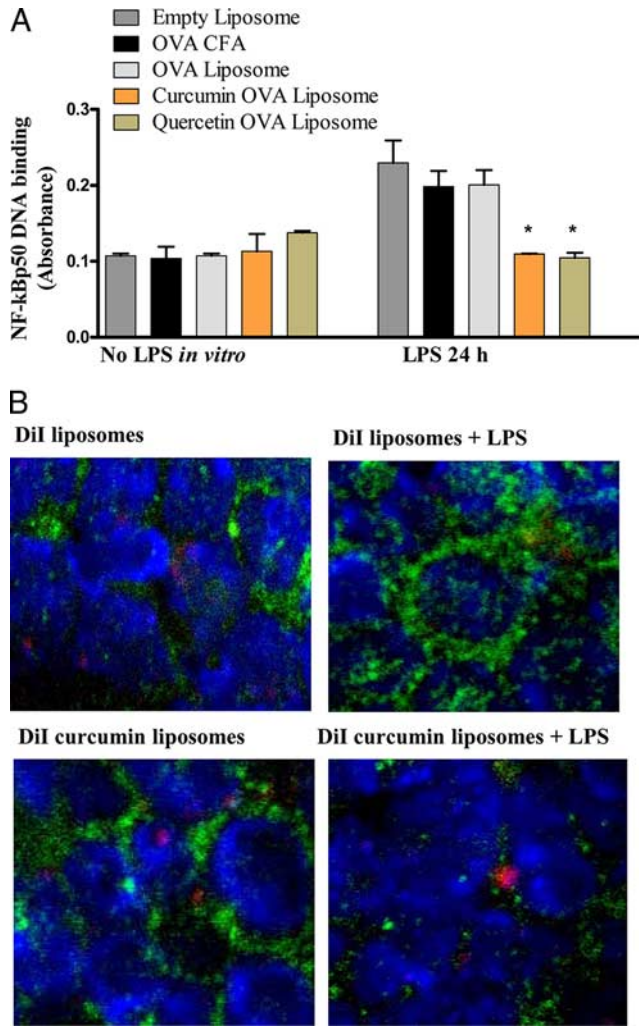
FIGURE 3. NF-κB activity is suppressed in spleen of mice administered liposomes encapsulating NF-κB inhibitors. Liposomes as indicated were injected i.v. and splenocytes were prepared 24 h later. *A*, After incubation for 24 h with or without LPS, nuclei were analyzed for p50/NF-κB DNA binding by ELISA. Each bar represents mean ± SD binding from three experiments, each containing pooled cells from three mice per group. *, $p < 0.05$, comparing LPS response after curcumin and quercetin-OVA liposomes with empty or OVA-liposomes or with OVA-CFA administration. *B*, After incubation for 3 h with or without LPS, splenocytes were fixed and analyzed by confocal microscopy at ×63 resolution. Cell nuclei (4′,6-diamidino-2-phenylindole) are blue, DiI-labeled liposomes are red, and NF-κB-p50 is green.

OVA/CFA after transfer of OVA-specific TCR-transgenic T cells. After 7 days, mice were injected s.c. with liposomes entrapping either OVA alone or OVA plus curcumin or with the adjuvant Quil A. After an additional 7 days, OVA-specific responses in the draining LNs were tested ex vivo. The OVA-specific response was suppressed following delivery of OVA-liposomes coentrapping curcumin, as compared with the response from OVA-CFA-primed mice or mice receiving OVA-QuilA liposomes. T cell proliferation was suppressed to a lesser extent by OVA-only liposomes than by OVA-liposomes coentrapping curcumin, presumably due to the targeting of OVA to resting APCs ($p < 0.05$; Fig. 5*A*) (24). Suppression of T cell proliferation was associated with reduced secretion of IL-2, TNF, and IFN-γ and increased secretion of IL-10 (Fig. 5*A*). These data indicate that Ag-specific responses can be suppressed in previously primed mice by delivery of liposomes coentrapping Ag and a NF-κB inhibitor. This phenomenon was
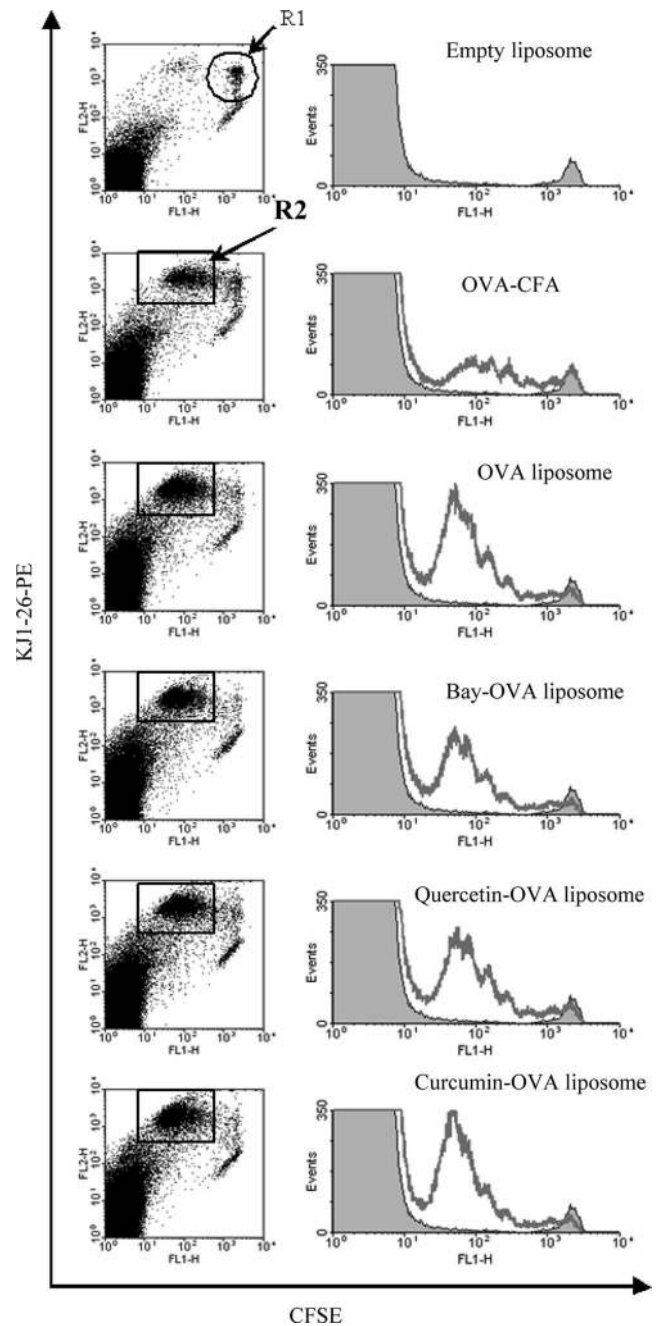

FIGURE 4. Liposomes deliver Ag to T cells in draining LN. Five × 10[6] CFSE-labeled DO11.10 OVA-specific T cells were transferred to BALB/c mice, followed 24 h later by s.c. (tail base) injection of OVA-CFA or 100 μl of OVA-liposomes formulated without inhibitor, or with Bay11-7082, curcumin, or quercetin. Seventy-two hours after OVA delivery, draining inguinal LNs were removed and cell suspensions were stained with PE-conjugated clonotypic KJ1-26 Ab, recognizing DO11.10 cells, then analyzed by flow cytometry. Dot plots with circular gate (R1) represent OVA-specific CFSE[high] parent T cells while dot plots with rectangular gate (R2) represent daughter T cells. (The small population below R1 contains autofluorescent LN macrophages.) Reduction in CFSE fluorescence intensity (from *right* to *left*) depicts OVA-specific T cell proliferation. Results are representative of two separate experiments.

associated with IL-10 production and suppression of proinflammatory cytokines in an Ag-specific manner.

To determine whether liposomes coentrapping OVA and NF-κB inhibitors induced Ag-specific Treg cells, we first tested whether Ag-specific FoxP3^{+} T cells were expanded in response to
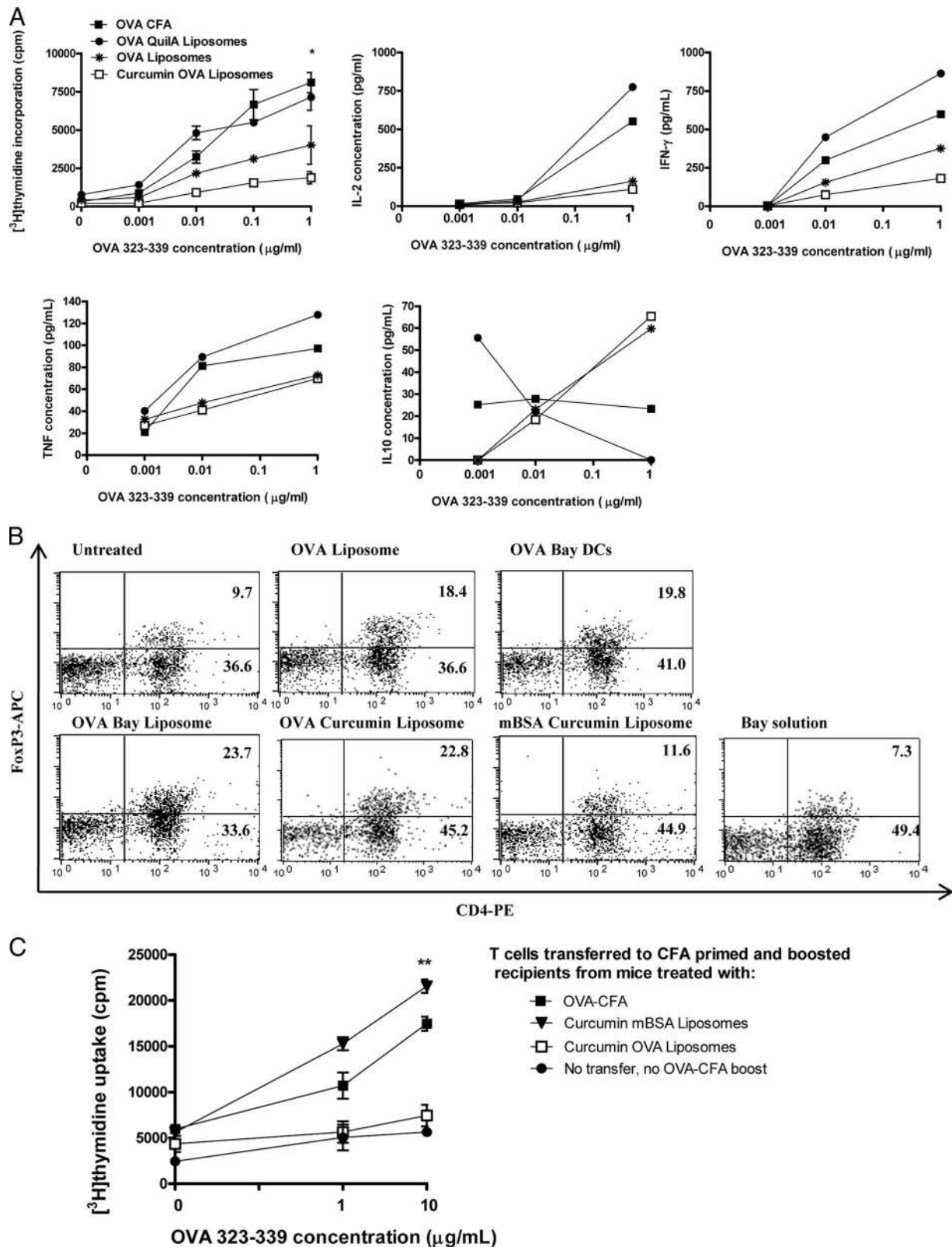
FIGURE 5. Liposomes coentrapping curcumin and Ag induce Ag-specific Treg cells. *A,* BALB/c mice were primed with OVA-CFA 24 h after adoptive transfer of DO11.10 T cells. After 7 days, OVA-CFA or s.c. liposomes, as shown, were administered. T cells were harvested from draining LN 7 days later and restimulated with OVA peptide as described in *Materials and Methods.* Mean cpm ± SEM from triplicate wells are shown. *, $p < 0.05$. The levels of IL-2, IFN-γ, TNF, and IL-10 were evaluated in pooled supernatants by cytokine bead array. *B,* BALB/c mice were primed with OVA-CFA 24 h after adoptive transfer of DO11.10 T cells. After 7 days, the following were injected s.c.: OVA-liposomes, OVA-Bay-DCs, OVA-Bay-liposomes, OVA-curcumin-liposomes, mBSA-curcumin-liposomes, or Bay solution and one group was untreated. Inguinal LN cells were stained 8 days later with CD4-PE and FoxP3-allophycocyanin. The percent CD4^{+} cells expressing FoxP3 is shown in the *upper right quadrant* of each histogram. *C,* C57BL/6 recipient mice were primed with OVA-CFA. Donor mice were injected s.c. with liposomes as shown, or left untreated, 24 h after adoptive transfer of OT-II T cells. After 7 days, T cells purified from each donor group were transferred to the primed recipients, and all of the groups were boosted with OVA-CFA. After 5 days, inguinal LN T cells were restimulated with OVA peptide. Results are representative of two separate experiments. **, $p < 0.01$.
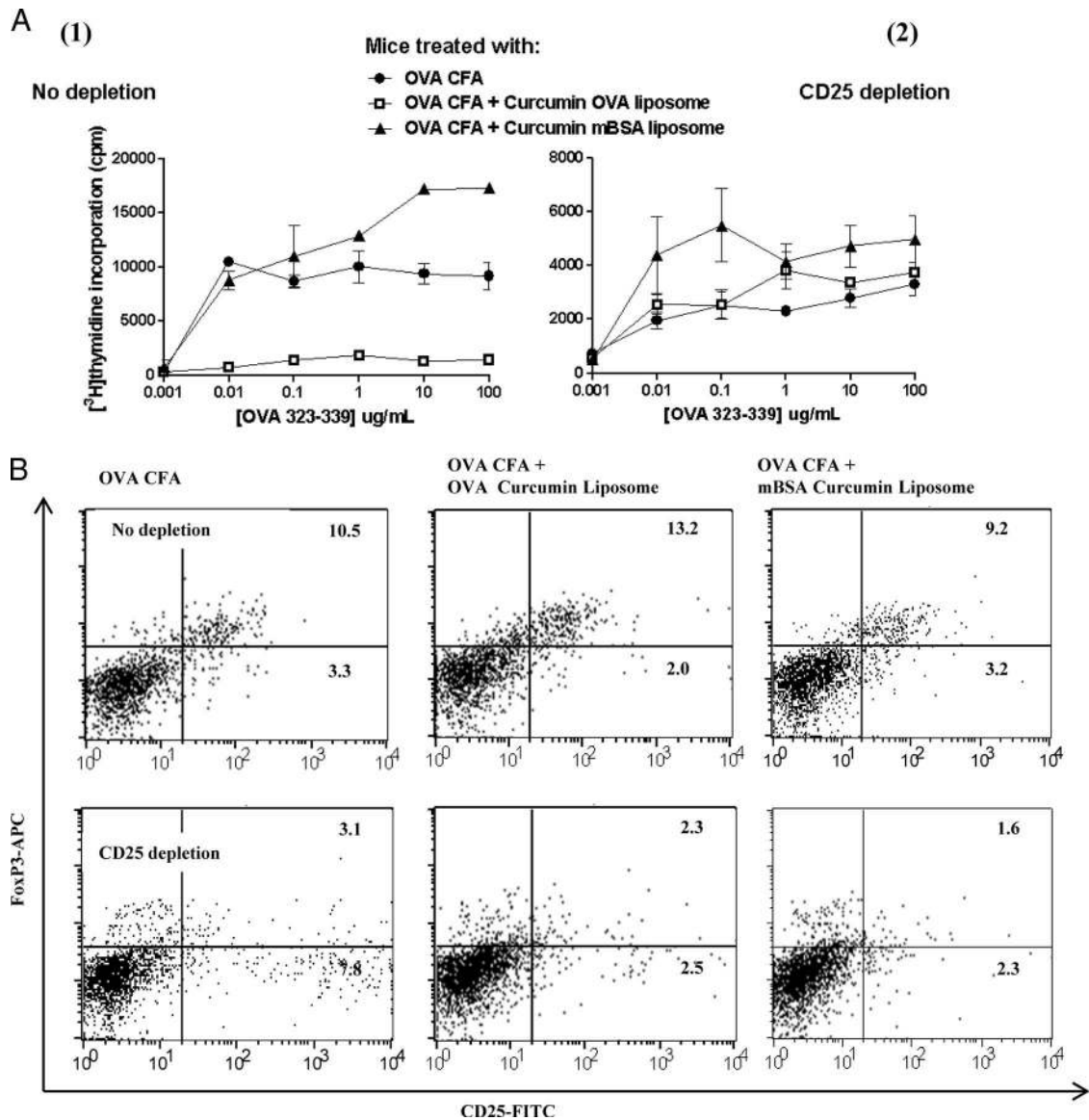
FIGURE 6. Liposomes coentrapping curcumin and Ag fail to induce suppression in the absence of $CD25^+$ T cells. DO11.10 T cells were adoptively transferred into two groups of BALB/c mice on day 0. Group 1 received $CD4^+$ T cells and group 2 received $CD25^-CD4^+$ DO11.10 T cells. Group 2 was treated with anti-CD25 mAb on days −1, 2, and 7. On day 1, mice from each group were treated s.c. with either no treatment, OVA-curcumin-liposomes, or mBSA-curcumin-liposomes. On day 8, all mice were primed with OVA-CFA. Seven days after priming, T cells were purified from draining inguinal LNs and restimulated with OVA peptide as described in *Materials and Methods* (*A*) or stained with anti-CD25 and anti-FoxP3, then analyzed by flow cytometry (*B*). The percent $CD25^+$ cells expressing FoxP3 is shown in the *upper right quadrant* of each histogram.

liposomes coentrapping Ag and a lipophilic NF-κB inhibitor and, second, used a mouse donor-recipient system. To determine $FoxP3^+$ T cell expansion and its Ag specificity, naive mice were primed with OVA-CFA 24 h after adoptive transfer of OVA-specific TCR-transgenic T cells. After 7 days, mice were injected s.c. with liposomes entrapping either OVA alone, OVA plus curcumin, OVA plus Bay 11-7082, mBSA plus curcumin, OVA-pulsed Bay-treated DCs, or Bay 11-7082 solution. One group of mice was untreated. Eight days after treatment with liposomes coentrapping OVA and either curcumin or Bay11-7082 or after delivery of OVA-pulsed Bay-treated DCs, the proportion of $CD4^+$ T cells expressing FoxP3 (or CD25 and FoxP3; data not shown) increased in draining LNs >2-fold (Fig. 5*B*). The proportion of $FoxP3^+$ $CD4^+$ Treg also increased after delivery of liposomes entrapping OVA alone, consistent with the reduction in OVA-specific T cell response observed after delivery of this formulation (Fig. 5*A*). However, the increase in Treg cell proportion in draining LNs was

Ag specific, as no increase was observed after delivery of liposomes entrapping mBSA and curcumin, or Bay solution in the absence of Ag (Fig. 5*C*).

For the mouse donor-recipient system, OVA-specific TCR-transgenic T cells were transferred to naive recipient mice. The mice were then primed with OVA-CFA. Donor mice were injected s.c. with curcumin liposomes coentrapping OVA. or curcumin liposomes coentrapping mBSA, or were left untreated. Seven days later, T cells purified from the donor mice were transferred to the primed recipient mice; all mice were boosted with OVA-CFA. After 5 days, OVA-specific responses in draining LNs were tested ex vivo. Transfer of T cells from mice injected with liposomes coentrapping OVA and curcumin suppressed OVA-specific responses in an Ag-specific fashion (relative to responses of mice primed and boosted with OVA-CFA or of mice injected with liposomes coentrapping mBSA and curcumin; $p < 0.01$, Fig. 5*C*).
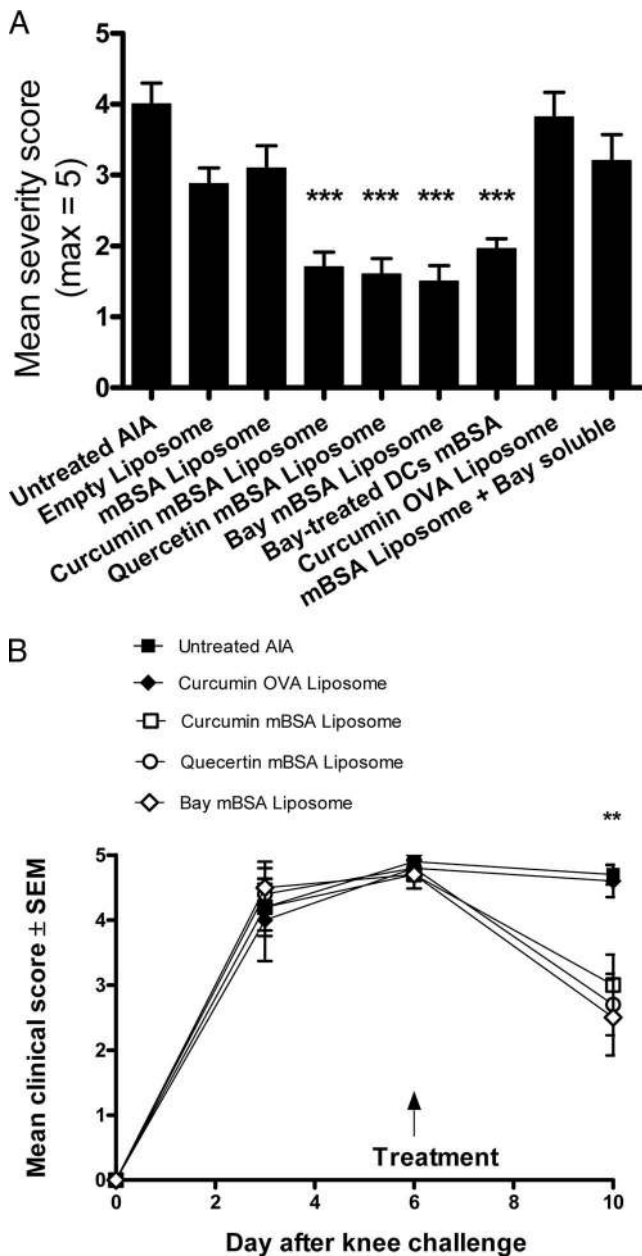
FIGURE 7. Suppression of Ag-induced arthritis in mice treated with liposomes coentrapping NF-κB inhibitor and mBSA. C57BL/6 mice were primed with mBSA, CFA, and pertussis toxin at day −21, and at day 0 mBSA was injected into one knee joint and saline to the other. Six days later, treatments as shown were injected s.c. into the tail base. Clinical scores were followed until sacrifice. After sacrifice on day 10, joints were graded for severity from 0 to 5 as described in *Materials and Methods*. A positive delayed-type hypersensitivity response was recorded in all mice with AIA. The mean severity score of control (saline-injected) joints was 0.5 ± 0 (SEM). Severity (*A*) and clinical (*B*) scores of mice with AIA either untreated or treated with empty liposomes, liposomes entrapping mBSA, liposomes coentrapping mBSA and curcumin, liposomes coentrapping mBSA and quercetin, liposomes coentrapping mBSA and Bay 11-7082, liposomes coentrapping OVA and curcumin, and liposomes entrapping mBSA with soluble Bay 11-7082 injected separately or with 5×10^5 mBSA-exposed bone marrow-derived DCs prepared in vitro in the presence of Bay11-7082. Results represent mean $\pm$ SEM from groups of at least 10 mice tested individually. **, $p < 0.005$ and ***, $p < 0.001$, compared with untreated mice.

Taken together, the data indicate that APC taking up liposomes coentrapping Ag and a lipophilic NF-κB inhibitor induce Ag-specific Treg cells, characterized by IL-10 production and FoxP3 expression, which suppress a previously primed immune response. We determined next whether CD25+FoxP3+ thymic-derived Treg were required for induction of Ag-specific Treg in naive mice by APC taking up liposomes coentrapping Ag and a lipophilic NF-κB inhibiton (Fig. 6). We treated one group of naive mice with anti-CD25 mAb every 3 days to deplete CD25+ cells. Control mice were untreated. Both groups received OVA-specific TCR-transgenic T cells. In the case of the group treated with anti-CD25, the adoptively transferred T cells were first depleted of CD25+ cells. The following day, mice from each group were injected s.c. with either curcumin liposomes coentrapping OVA, or curcumin liposomes coentrapping mBSA, or were left untreated. One week later, all mice were primed with OVA-CFA. Seven days after priming, OVA-specific responses in draining LNs were tested ex vivo. As expected, the OVA-specific effector T cell response to OVA priming was reduced in the group depleted of CD25+ cells. However, we did not observe the Ag-specific suppression afforded by delivery of curcumin liposomes coentrapping OVA when CD25+ cells were depleted. Only 1–3% of draining LN cells expressed CD25 and FoxP3 in these mice at the completion of the experiment. These data are consistent with the conclusion that Ag-specific FoxP3+ Treg are induced by APC taking up liposomes coentrapping Ag and a lipophilic NF-κB inhibitor through a process which requires instruction by thymic-derived CD25+ Treg cells (25, 26).

Ag-specific suppression of Ag-induced arthritis using liposomes

To determine the effect of this novel system for codelivery of Ag and NF-κB inhibitor on the clinical severity of inflammatory arthritis, liposomes were delivered to mice with AIA (27). AIA was chosen as a model because its clinical features resemble RA and because it has a defined arthritogenic Ag, mBSA, to which tolerance can be induced using DCs in vivo (9). Six days after AIA induction (when disease was fully established), liposomes coentrapping mBSA and NF-κB inhibitors were injected s.c. After sacrifice, joint severity scores demonstrated that arthritis was reduced after injection of liposomes coentrapping mBSA and NF-κB inhibitors ($p < 0.001$; Fig. 7A). Reductions in swelling were Ag specific, as liposomes coentrapping OVA and curcumin did not suppress arthritis. We also tested whether codelivery of Ag and NF-κB inhibitor in the same liposome was essential for treatment efficacy. Mice were treated with liposomes entrapping curcumin administered concurrently with s.c. mBSA solution or mBSA liposomes administered concurrently with Bay11-7082 solution s.c. Arthritis severity was reduced after delivery of liposomes coentrapping mBSA and a NF-κB inhibitor but not after separate delivery of liposomes and Bay11-7082 (Fig. 7A). Knee joint swelling subsided within 4 days of injection of liposomes coentrapping mBSA and NF-κB inhibitors or mBSA-exposed RelB^low DCs (all compared with untreated mice; $p < 0.005$, Fig. 7B).

Discussion

We demonstrated that liposomes encapsulating Ag and a lipophilic NF-κB inhibitor target APCs in situ to induce Ag-specific tolerance in mice. The Ag specificity and efficacy of immune suppression was similar to that achieved with Ag-loaded modified autologous DCs generated ex vivo in the presence of the NF-κB inhibitor Bay11-7082, which we previously found to be similar to the suppression achieved with a TNF inhibitor (7, 9). IL-10-producing FoxP3+ Ag-specific Treg were induced, instructed by CD25+ thymic-derived Treg cells, by lymphoid organ APC-presenting Ag codelivered with NF-κB inhibitor. These Treg cells induced Ag-specific tolerance, suppressing full-blown AIA in an

Ag-specific manner. Ag-specific Treg induced by transferred RelB[low] DCs were shown to express FoxP3 and to suppress immunity in an IL-10-dependent manner (7, 9, 28).

NF-κB inhibitors, such as curcumin, also block innate immunity. However, our data demonstrate that treatment with loaded liposomes depends on the action of CD25^{+} T cells and that targeting NF-κB inhibitors alone to phagocytic cells is insufficient to induce FoxP3^{+} Treg cells or to suppress AIA, e.g., by suppression of innate immunity (including secretion of proinflammatory cytokines and increased expression of adhesion molecules). This is because neither Bay11-7082 alone, curcumin liposomes containing irrelevant Ag, nor curcumin liposomes and soluble arthritogenic Ag administered concurrently were sufficient to induce FoxP3^{+} Treg cells or to suppress arthritis. Rather, we and others have shown that blocking RelB activity inhibits functional DC differentiation, with induction of Treg specific for delivered Ag (7, 28, 29).

To promote Ag-specific tolerance, liposomes must deliver their payload to phagocytic APCs that are resident in, or migrate to, lymphoid organs (30). Our data indicate that liposomes entrapping quercetin or curcumin efficiently block NF-κB nuclear translocation and DNA binding in targeted APCs in vivo. Our flow cytometric and microscopy studies indicate that liposome-loaded APCs (e.g., macrophages and several DC subtypes) are viable in situ.

The described liposome encapsulation technique offers flexibility in terms of Ags, particles, and inhibitors for delivery of Ag-specific tolerizing immunotherapy. Since no targeting Abs are involved, it can be readily translated from murine studies to human clinical trials (23). Liposomes also allow the encapsulation of immunomodulators besides curcumin or quercetin. Hydrophobic aliphatic chains of phospholipids form the interior of the liposome bilayer and can solubilize or entrap a wide range of lipophilic molecules. Liposome stability in vivo can be altered by modifying the lipid composition, e.g., addition of cholesterol.

The activity of curcumin has been shown to increase when it is formulated in liposomes, at least in vitro and in animal tumor models (31, 32). The use of liposomes and the phagocytic capacity of APCs to target curcumin efficiently takes advantage of curcumin's immunomodulatory properties. Moreover, curcumin has low toxicity when delivered orally in mouse models and in a phase I clinical trial (31, 33). In the current studies, delivery of curcumin-liposomes to lymphoid organ APCs did not promote death or other obvious toxic effects to the targeted cells. Preliminary experiments in a model of viral infection also showed no adverse effect of curcumin-liposomes, when delivered at the time of infection, on the kinetics of viral clearance. Although curcumin is a very potent NF-κB inhibitor, it has additional immunomodulatory properties including antioxidant effects (13, 34, 35). Its effects on targeted APCs are reproduced, however, by the specific NF-κB inhibitor Bay11-7082 (12), when coencapsulated with Ag in liposomes. Curcumin and quercetin had the advantage of increased liposome entrapment efficiency of 80–90% as a result of their greater lipophilicity, compared with the less lipophilic Bay 11-7082, with entrapment efficiency of 45–65%.

RA is an ideal disease target for Ag-specific immunotherapy. This disease affects 1% of the global population, reducing life expectancy in this group by an average of 10 years; the direct medical cost of RA to the U.S. health system exceeds $90,000 per patient per annum. Citrullinated proteins represent an important group of RA autoantigens in patients carrying HLA susceptibility genotypes (36). Inflammatory arthritis can be induced by priming mice transgenic for a RA HLA susceptibility allele with citrullinated fibrinogen (37). In another mouse model of autoimmune arthritis, disease severity was reduced after injection of a citrulline-containing peptide to induce tolerance, compared with controls (38).

Thus, liposomes loaded with citrullinated proteins could be harnessed as delivery vehicles for Ag-specific tolerance in genetically susceptible patients with autoantibodies reactive to citrullinated self-Ags. Liposomes have the potential to entrap Ags associated with other autoimmune diseases besides RA and might be used for individualized treatment of allergies and organ rejection after transplant, thus reducing the need for systemic immunosuppression or biologic therapies that have unpleasant and dangerous side effects.

Disclosures

The authors have no financial conflict of interest.

References

1. Wolfe, F., K. Michaud, B. Stephenson, and J. Doyle. 2003. Toward a definition and method of assessment of treatment failure and treatment effectiveness: the case of leflunomide versus methotrexate. *J. Rheumatol.* 30: 1725–1732.
2. Hyrich, K. L., M. Lunt, W. G. Dixon, K. D. Watson, and D. P. Symmons. 2008. Effects of switching between anti-TNF therapies on HAQ response in patients who do not respond to their first anti-TNF drug. *Rheumatology* 47: 1000–1005.
3. Schellekens, G. A., H. Visser, B. A. de Jong, F. H. van den Hoogen, J. M. Hazes, F. C. Breedveld, and W. J. van Venrooij. 2000. The diagnostic properties of rheumatoid arthritis antibodies recognizing a cyclic citrullinated peptide. *Arthritis Rheum.* 43: 155–163.
4. Dittel, B. N., I. Visintin, R. M. Merchant, and C. A. Janeway, Jr. 1999. Presentation of the self antigen myelin basic protein by dendritic cells leads to experimental autoimmune encephalomyelitis. *J. Immunol.* 163: 32–39.
5. Lutzky, V., S. Hannawi, and R. Thomas. 2007. Cells of the synovium in rheumatoid arthritis: dendritic cells. *Arthritis Res. Ther.* 9: 219.
6. O'Sullivan, B. J., and R. Thomas. 2002. CD40 ligation conditions dendritic cell antigen-presenting function through sustained activation of NF-κB. *J. Immunol.* 168: 5491–5498.
7. Martin, E., B. J. O'Sullivan, P. Low, and R. Thomas. 2003. Antigen-specific suppression of a primed immune response by dendritic cells mediated by regulatory T cells secreting interleukin-10. *Immunity* 18: 155–167.
8. Thompson, A. G., B. J. O'Sullivan, H. Beamish, and R. Thomas. 2004. T cells signaled by NF-κB-dendritic cells are sensitized not anergic to subsequent activation. *J. Immunol.* 173: 1671–1680.
9. Martin, E., C. Capini, E. Duggan, V. P. Lutzky, P. Stumbles, A. R. Pettit, B. O'Sullivan, and R. Thomas. 2007. Antigen-specific suppression of established arthritis in mice by dendritic cells deficient in NF-κB. *Arthritis Rheum.* 56: 2255–2266.
10. Claassen, E. 1992. Post-formation fluorescent labelling of liposomal membranes: in vivo detection, localisation and kinetics. *J. Immunol. Methods* 147: 231–240.
11. Pettit, A. R., C. Quinn, K. P. MacDonald, L. L. Cavanagh, G. Thomas, W. Townsend, M. Handel, and R. Thomas. 1997. Nuclear localization of RelB is associated with effective antigen-presenting cell function. *J. Immunol.* 159: 3681–3691.
12. Pierce, J. W., R. Schoenleber, G. Jesmok, J. Best, S. A. Moore, T. Collins, and M. E. Gerritsen. 1997. Novel inhibitors of cytokine-induced IκBα phosphorylation and endothelial cell adhesion molecule expression show anti-inflammatory effects in vivo. *J. Biol. Chem.* 272: 21096–21103.
13. Kim, G. Y., K. H. Kim, S. H. Lee, M. S. Yoon, H. J. Lee, D. O. Moon, C. M. Lee, S. C. Ahn, Y. C. Park, and Y. M. Park. 2005. Curcumin inhibits immunostimulatory function of dendritic cells: MAPKs and translocation of NF-κB as potential targets. *J. Immunol.* 174: 8116–8124.
14. Kim, B. H., S. M. Cho, A. M. Reddy, Y. S. Kim, K. R. Min, and Y. Kim. 2005. Down-regulatory effect of quercitrin gallate on nuclear factor-κB-dependent inducible nitric oxide synthase expression in lipopolysaccharide-stimulated macrophages RAW 264.7. *Biochem. Pharmacol.* 69: 1577–1583.
15. Pulendran, B., J. Lingappa, M. K. Kennedy, J. Smith, M. Teepe, A. Rudensky, C. R. Maliszewski, and E. Maraskovsky. 1997. Developmental pathways of dendritic cells in vivo: distinct function, phenotype, and localization of dendritic cell subsets in FLT3 ligand-treated mice. *J. Immunol.* 159: 2222–2231.
16. Vremec, D., M. Zorbas, R. Scollay, D. J. Saunders, C. F. Ardavin, L. Wu, and K. Shortman. 1992. The surface phenotype of dendritic cells purified from mouse thymus and spleen: investigation of the CD8 expression by a subpopulation of dendritic cells. *J. Exp. Med.* 176: 47–58.
17. Vremec, D., J. Pooley, H. Hochrein, L. Wu, and K. Shortman. 2000. CD4 and CD8 expression by dendritic cell subtypes in mouse thymus and spleen. *J. Immunol.* 164: 2978–2986.
18. Nakano, H., M. Yanagita, and M. D. Gunn. 2001. CD11c^{+}B220^{+}Gr-1^{+} cells in mouse lymph nodes and spleen display characteristics of plasmacytoid dendritic cells. *J. Exp. Med.* 194: 1171–1178.
19. Blasius, A. L., E. Giurisato, M. Cella, R. D. Schreiber, A. S. Shaw, and M. Colonna. 2006. Bone marrow stromal cell antigen 2 is a specific marker of type I IFN-producing cells in the naive mouse, but a promiscuous cell surface antigen following IFN stimulation. *J. Immunol.* 177: 3260–3265.
20. Bonifaz, L., D. Bonnyay, K. Mahnke, M. Rivera, M. C. Nussenzweig, and R. M. Steinman. 2002. Efficient targeting of protein antigen to the dendritic cell

receptor DEC-205 in the steady state leads to antigen presentation on major histocompatibility complex class I products and peripheral CD8^{+} T cell tolerance. *J. Exp. Med.* 196: 1627–1638.

21. Hawiger, D., K. Inaba, Y. Dorsett, M. Guo, K. Mahnke, M. Rivera, J. V. Rauetch, R. M. Steinman, and M. C. Nussenzweig. 2001. Dendritic cells induce peripheral T cell unresponsiveness under steady state conditions in vivo. *J. Exp. Med.* 194: 769–780.

22. Lohr, J., B. Knoechel, E. C. Kahn, and A. K. Abbas. 2004. Role of B7 in T cell tolerance. *J. Immunol.* 173: 5028–5035.

23. Mahnke, K., Y. Qian, J. Knop, and A. H. Enk. 2003. Induction of CD4^{+}/CD25^{+} regulatory T cells by targeting of antigens to immature dendritic cells. *Blood* 101: 4862–4869.

24. Steptoe, R. J., J. M. Ritchie, N. S. Wilson, J. A. Villadangos, A. M. Lew, and L. C. Harrison. 2007. Cognate CD4^{+} help elicited by resting dendritic cells does not impair the induction of peripheral tolerance in CD8^{+} T cells. *J. Immunol.* 178: 2094–2103.

25. Dieckmann, D., C. H. Bruett, H. Ploettner, M. B. Lutz, and G. Schuler. 2002. Human CD4^{+}CD25^{+} regulatory, contact-dependent T cells induce interleukin 10-producing, contact-independent type 1-like regulatory T cells [corrected]. *J. Exp. Med.* 196: 247–253.

26. Zheng, S. G., J. H. Wang, J. D. Gray, H. Soucier, and D. A. Horwitz. 2004. Natural and induced CD4^{+}CD25^{+} cells educate CD4^{+}CD25^{−} cells to develop suppressive activity: the role of IL-2, TGF-β, and IL-10. *J. Immunol.* 172: 5213–5221.

27. Brackertz, D., G. Mitchell, and I. R. Mackay. 1977. Antigen-induced arthritis in mice. *Arthritis Rheum.* 20: 841–850.

28. Li, M., X. Zhang, X. Zheng, D. Lian, Z. X. Zhang, W. Ge, J. Yang, C. Vladau, M. Suzuki, D. Chen, et al. 2007. Immune modulation and tolerance induction by RelB-silenced dendritic cells through RNA interference. *J. Immunol.* 178: 5480–5487.

29. Moore, F., S. Buonocore, E. Aksoy, N. Ouled-Haddou, S. Goriely, E. Lazarova, F. Paulart, C. Heirman, E. Vaeremans, K. Thielemans, et al. 2007. An alternative pathway of NF-κB activation results in maturation and T cell priming activity of dendritic cells overexpressing a mutated IκBα. *J. Immunol.* 178: 1301–1311.

30. Oussoren, C., M. Velinova, G. Scherphof, J. J. van der Want, N. van Rooijen, and G. Storm. 1998. Lymphatic uptake and biodistribution of liposomes after subcutaneous injection: IV. Fate of liposomes in regional lymph nodes. *Biochim. Biophys. Acta* 1370: 259–272.

31. Li, L., B. Ahmed, K. Mehta, and R. Kurzrock. 2007. Liposomal curcumin with and without oxaliplatin: effects on cell growth, apoptosis, and angiogenesis in colorectal cancer. *Mol. Cancer Ther.* 6: 1276–1282.

32. Thangapazham, R. L., A. Puri, S. Tele, R. Blumenthal, and R. K. Maheshwari. 2008. Evaluation of a nanotechnology-based carrier for delivery of curcumin in prostate cancer cells. *Int. J. Oncol.* 32: 1119–1123.

33. Sharma, R. A., S. A. Euden, S. L. Platton, D. N. Cooke, A. Shafayat, H. R. Hewitt, T. H. Marczylo, B. Morgan, D. Hemingway, S. M. Plummer, et al. 2004. Phase I clinical trial of oral curcumin: biomarkers of systemic activity and compliance. *Clin. Cancer Res.* 10: 6847–6854.

34. Sandur, S. K., M. K. Pandey, B. Sung, K. S. Ahn, A. Murakami, G. Sethi, P. Limtrakul, V. Badmaev, and B. B. Aggarwal. 2007. Curcumin, demethoxycurcumin, bisdemethoxycurcumin, tetrahydrocurcumin and turmerones differentially regulate anti-inflammatory and anti-proliferative responses through a ROS-independent mechanism. *Carcinogenesis* 28: 1765–1773.

35. Strasser, E. M., B. Wessner, N. Manhart, and E. Roth. 2005. The relationship between the anti-inflammatory effects of curcumin and cellular glutathione content in myelomonocytic cells. *Biochem. Pharmacol.* 70: 552–559.

36. van der Helm-van Mil, A. H., K. N. Verpoort, F. C. Breedveld, T. W. Huizinga, R. E. Toes, and R. R. de Vries. 2006. The HLA-DRB1 shared epitope alleles are primarily a risk factor for anti-cyclic citrullinated peptide antibodies and are not an independent risk factor for development of rheumatoid arthritis. *Arthritis Rheum.* 54: 1117–1121.

37. Hill, J. A., D. A. Bell, W. Brintnell, D. Yue, B. Wehrli, A. M. Jevnikar, D. M. Lee, W. Hueber, W. H. Robinson, and E. Cairns. 2008. Arthritis induced by posttranslationally modified (citrullinated) fibrinogen in DR4-IE transgenic mice. *J. Exp. Med.* 205: 967–979.

38. Kuhn, K. A., L. Kulik, B. Tomooka, K. J. Braschler, W. P. Arend, W. H. Robinson, and V. M. Holers. 2006. Antibodies against citrullinated proteins enhance tissue injury in experimental autoimmune arthritis. *J. Clin. Invest.* 116: 961–973.